

Electronic Supplementary Information

Synthesis and Charge-Transport Properties of

Novel π -Conjugated Polymers Incorporating Core-Extended Naphtho[2,1-*b*:3,4-*b'*]dithiophene Diimides

Lingli Zhao^{a,#}, Yanyan Cao^{b,#}, Hanwen Qin^a, Xi He^a, Zhiyuan Zhao^{b,*}, Yunlong Guo^b, Huajie Chen^{a,*}

^aKey Laboratory of Environmentally Friendly Chemistry and Applications of Ministry of Education, College of Chemistry, Xiangtan University, Xiangtan 411105, China. E-mail: chenhjoe@163.com

^bBeijing National Laboratory for Molecular Sciences, Key Laboratory of Organic Solids, Institute of Chemistry, Chinese Academy of Sciences, Beijing 100190, China. E-mail: zhaozhiyuan@iccas.ac.cn

[#]L. Zhao and Y. Cao contributed equally to this work.

1. Measurement

The ¹H and ¹³C NMR spectra were collected on a Bruker AVANCE 400 using tetramethylsilane (TMS) as the interval standard. Fourier transform infrared spectroscopy (FT-IR) was recorded on a NICOLET 6700 spectrometer in the range from 600 to 4000 cm⁻¹. Thermogravimetric analysis (TGA) was recorded on a TGA Q50 V20.13 Build 39 with a heating rate of 20 °C min⁻¹ from 25 to 600 °C. Differential scanning calorimetry (TA Instruments DSC-25) was conducted for thermal transition from 25 to 400 °C at a heating rate of 20 °C min⁻¹. Mass Spectrometry (MALDI-TOF-MS) was measured on an Orbitrap Fusion Lumos instrument. Liquid Chromatograph Mass Spectrometer (LC-MS) were determined on Agilent 1260 Infinity II LC System and Agilent 6230B TOF. High-temperature (150 °C) gel-permeation chromatography were conducted on a Agilent GPC instrument (Polymer Labs PL 220 system), which adopted 1,2,4-trichlorobenzene and polystyrene as the eluent and standard sample, respectively. UV-Vis absorption spectra of all the samples in the chloroform solutions and as the thin films casted onto the quartz glass were measured on an Agilent Cary 60 UV-Vis spectrophotometer. Cyclic voltammetry (CV) was performed on an electrochemistry workstation (CHI660E, Chen hua Shanghai) using a three-electrode cell system. To examine small molecule 4a, the electrochemical cell

contains a glassy carbon electrode, a Pt wire, and an Ag/AgCl (KCl, Sat'd) electrode. To characterize the redox potentials of both polymers, a Pt disk coated with polymer film, a Pt wire, and an Ag/AgCl (KCl, Sat'd) electrode were used as the working electrode, counter electrode, and reference electrode, respectively. Anhydrous and N₂-saturated tetrabutylammonium hexafluorophosphate (TBAPF₆, 0.1 M) solutions in chloroform and in acetonitrile were used as the supporting electrolytes to measure small molecules and polymers, respectively.

Under room temperature, a suitable single crystal of 4a was obtained by slow evaporation of the corresponding solution in CH₂Cl₂: petroleum ether (V: V = 1:10). Single-crystal X-ray data was collected on a XtaLAB AFC12 (RINC): Kappa single diffractometer using graphite-monochromated Cu K α radiation ($\lambda = 1.54184 \text{ \AA}$). Using Olex2^[1], the structures were solved with the SHELXS ^[2] structure solution program using Direct Methods and refined with the SHELXL ^[3] refinement package using Least Squares minimization.

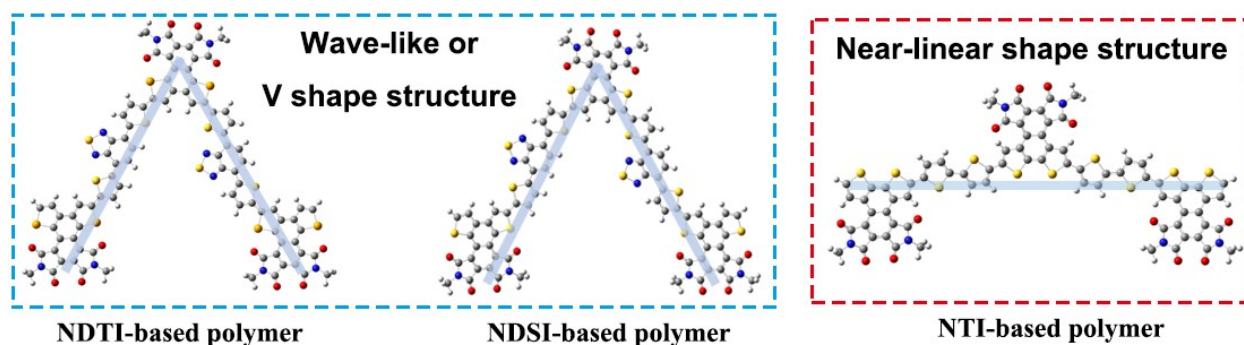


Fig. S1 Ground-state geometries of NDTI-/ NDSI-based polymer models and NTI-based polymer model calculated at the level of B3LYP/6-31G.

2. GPC characterization

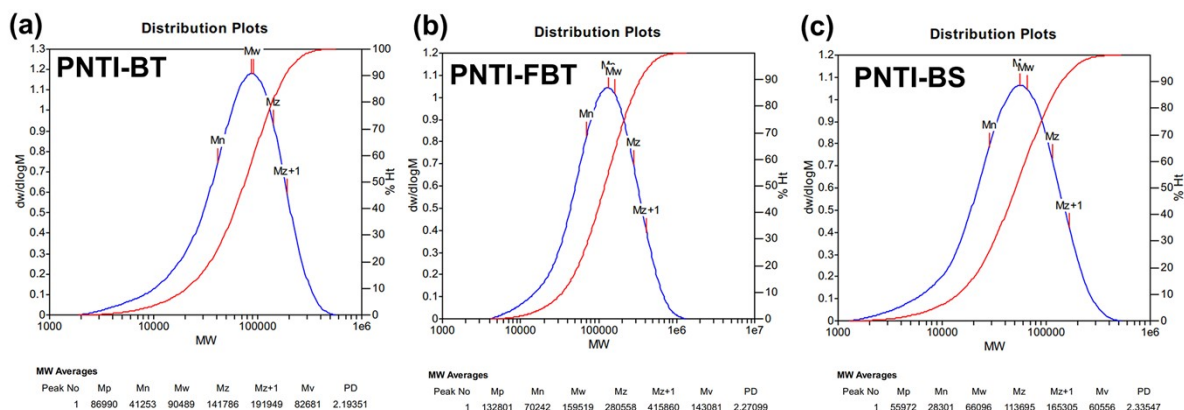


Fig. S2 GPC curves of the NTI-based copolymers.

3. DSC characterization

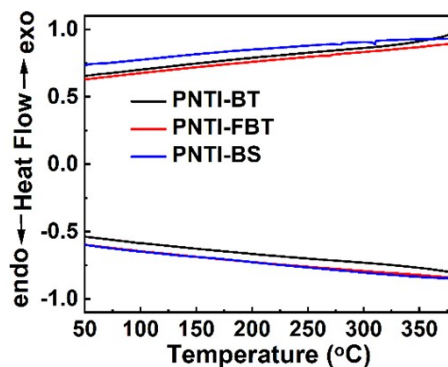


Fig. S3 DSC curves of the NTI-based copolymers under N₂ atmosphere.

4. TGA characterization

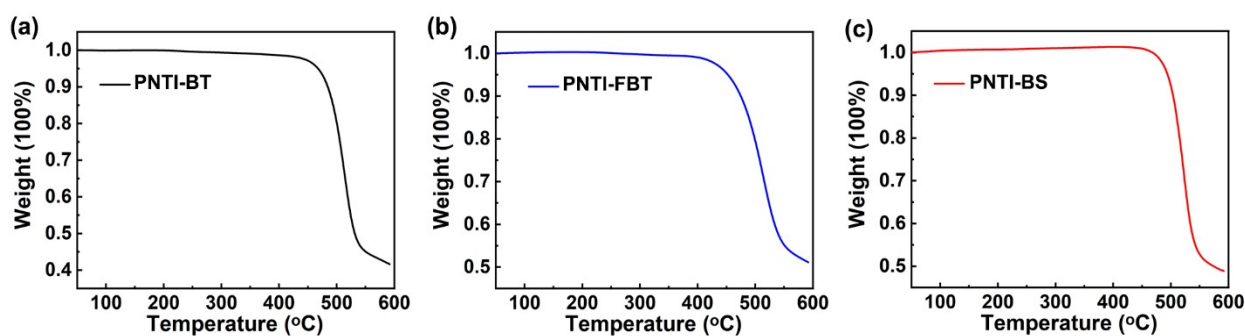


Fig. S4 TGA curves of the NTI-based copolymers under N₂ atmosphere.

5. FT-IR spectrometer

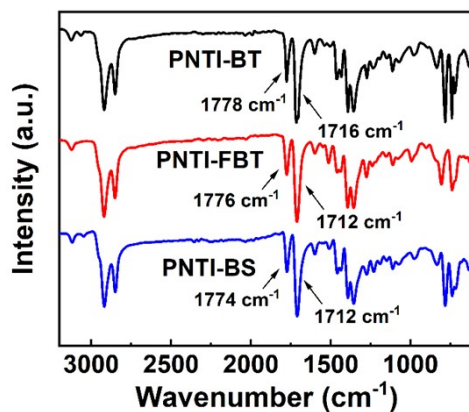


Fig. S5 FT-IR spectra of the NTI-based copolymers.

6. Comparison of ^1H NMR signals

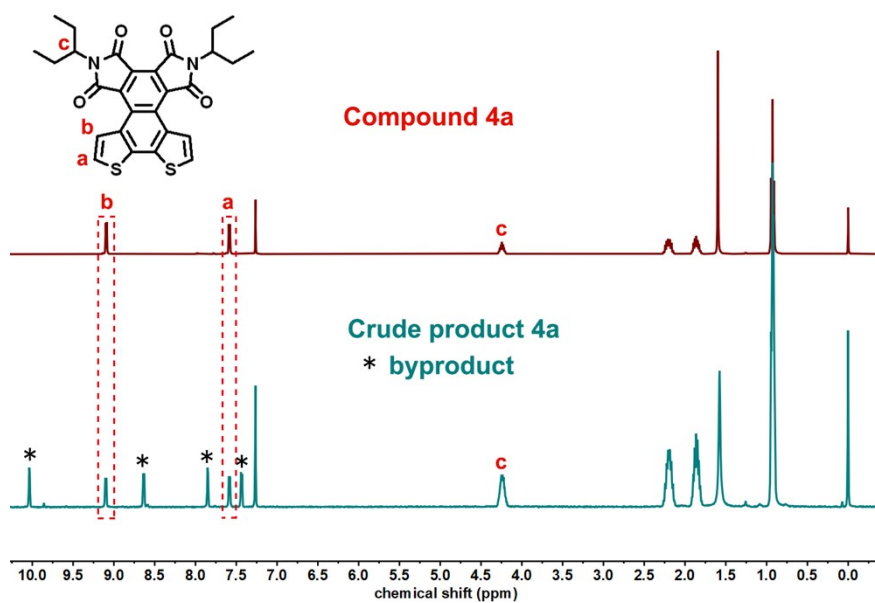


Fig. S6 Comparison of ^1H NMR signals between the compound 4a and the crude product of 4a and a few byproducts.

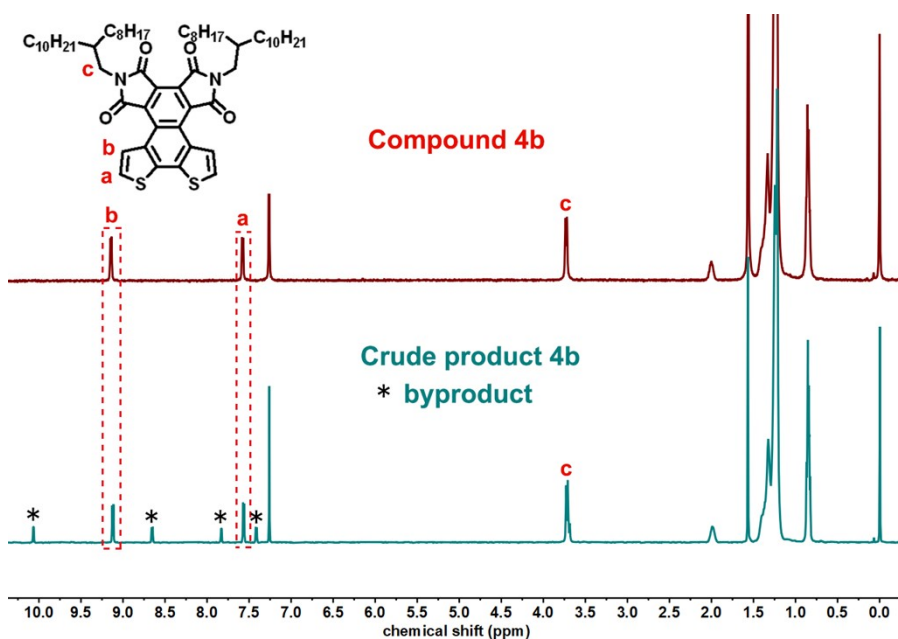


Fig. S7 Comparison of ^1H NMR signals between the compound 4b and the crude product of 4b and a few byproducts.

7. Single Crystal Parameters

Table S1 Crystal data and structure refinement for 4a

Identification code	4a
Empirical formula	C ₂₈ H ₂₄ Br ₂ N ₂ O ₄ S ₂
Formula weight	676.43
Temperature/K	150.00(10)
Crystal system	monoclinic
Space group	P2 ₁ /c
a/Å	15.37851(9)
b/Å	22.32456(14)
c/Å	7.70669(5)
α/°	90
β/°	91.6555(5)
γ/°	90
Volume/Å ³	2644.74(3)
Z	4
ρ _{calc} /g/cm ³	1.699
μ/mm ⁻¹	5.692
F(000)	1360.0
Crystal size/mm ³	0.14 × 0.12 × 0.11
Radiation	Cu Kα (λ = 1.54184)
2θ range for data collection/°	5.75 to 133.2
Index ranges	-18 ≤ h ≤ 18, -26 ≤ k ≤ 26, -9 ≤ l ≤ 5
Reflections collected	25803
Independent reflections	4680 [R _{int} = 0.0262, R _{sigma} = 0.0176]
Data/restraints/parameters	4680/45/405
Goodness-of-fit on F ²	1.041
Final R indexes [I ≥ 2σ (I)]	R ₁ = 0.0271, wR ₂ = 0.0722
Final R indexes [all data]	R ₁ = 0.0286, wR ₂ = 0.0732
Largest diff. peak/hole / e Å ⁻³	0.63/-0.41
CCDC number	2302738

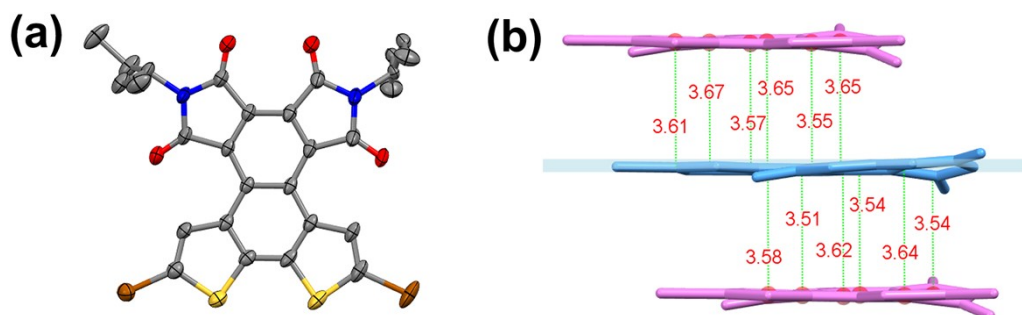


Fig. S8 (a) Thermal ellipsoid plot of 4a at the 50% probability level. Nitrogen, sulfur, oxygen, and carbon atoms are indicated as blue, yellow, red, and gray color, respectively. The hydrogen atoms are omitted for clarify; (b) Crystal packing distances determined from the adjacent molecules.

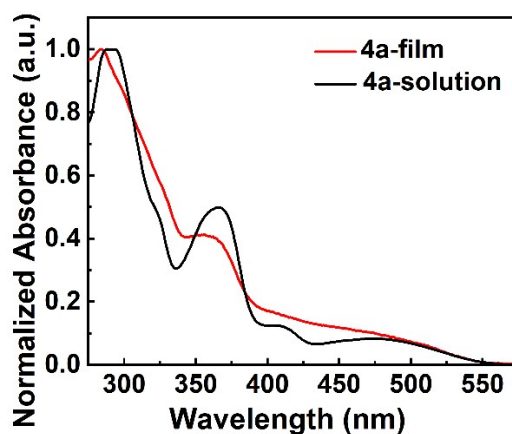


Fig. S9 Normalized absorption spectra of the NTI-based model compound 4a in CHCl_3 solution and as thin film.

8. DFT Calculations

To gain deeper insight to the chemical properties of model compounds 4a and polymer PNTI-BT, PNTI-FBT and PNTI-BS, density functional theory (DFT) calculations and time-dependent DFT (TD-DFT) were conducted by using Gaussian 09 program [4]. For 4a, both the structural optimization and frequency analysis calculation were carried out at B3LYP/6-31G level of theory. To get the optimized structure of PNTI-BT, PNTI-FBT and PNTI-BS, 2.5 repeat units were choose to do computation at

B3LYP/6-31G level of theory [5]. The UV-Vis absorption spectra of 4a were performed via time-dependent density functional theory (TD-DFT) calculation at PBE0/Def2TZVP level of theory. The solvent effect of CHCl₃ was taken into consideration by a polarizable continuum model [6].

Table S2 Theoretical simulation spectral data of 4a

compound	Excited States	Energy (eV)	Wavelength (nm)	Osc. Strength	Main contributions
4a	1	2.1924	565.52	0.06610	HOMO→LUMO 98.7%
	3	3.1948	388.08	0.36280	HOMO-1→LUMO 74.0% HOMO→LUMO+1 15.3%
	12	3.9296	315.51	0.52740	HOMO→LUMO+2 51.8% HOMO-1→LUMO+1 36.5% HOMO-7→LUMO 6.8%
	14	4.1096	301.69	0.07270	HOMO-7→LUMO 76.7% HOMO-5→LUMO 9.5% HOMO-1→LUMO+1 5.7%
	15	4.1352	299.83	0.16320	HOMO-6 →LUMO 73.4% HOMO-2 →LUMO+1 18.1%
	16	4.2466	291.96	0.17390	HOMO→LUMO+3 74.5% HOMO→LUMO+4 8.8% HOMO-1→LUMO+2 8.2%
	18	4.4603	277.97	0.05360	HOMO-3→LUMO+1 74.6% HOMO-13→LUMO 7.8%

9. OFET transistor device fabrication

To evaluate the charge transport performance of the NTI-based polymers, organic field-effect transistors (OFETs) with a top-gate/bottom-contact architecture were fabricated on the glass (300 nm) substrate. The source/drain (S/D) electrodes (30 nm Au) were deposited on the the surface of glass substrates by using a standard photolithography technique, with the corresponding channel length (L) of 40 μm and width (W) of 4500 μm . The substrates were washed by ultrasonication in acetone and isopropanol, followed by the treatment with UV-O₃. After that, the Au S/D electrodes was modified with pentafluorothiophenol (PFBT) according to the reported methods [7]. The semiconductor layer

was deposited on the surface of the PFBT-modified glass substrates by spin-coating a polymer solution in *o*-dichlorobenzene (10 mg mL⁻¹) at a rotation speed of 3000 rpm for 60 s, followed by the thermal treatment in a vacuum oven at 180 °C for 10 min. Next, a polymethyl methacrylate (PMMA, $M_w = 99.6$ kDa) solution in anhydrous *n*-butyl acetate (70 mg mL⁻¹) was spin-coated onto the surface of the semiconducting film. The thickness and dielectric constant of PMMA were determined as around 1000 nm and 2.7, respectively. The samples were further dried at 90°C for 1 h in a vacuum oven in order to remove the organic solvent in the film. Finally, the aluminum gate electrodes (~100 nm) were evaporated onto the surface of the PMMA gate dielectric by using a shadow mask technique. All the devices were measured in ambient air. The electrical characteristics were measured using a Keithley 4200A-SCS Parameter analyzer. The saturation mobility was calculated using the transistor equation:

$$I_{DS} = (W/2L) C_i \mu (V_G - V_T)^2$$

Where C_i represents the capacitance of the gate dielectric; V_G and V_T represent the gate voltage and the threshold voltage, respectively.

10. 1D-GIXRD characterization

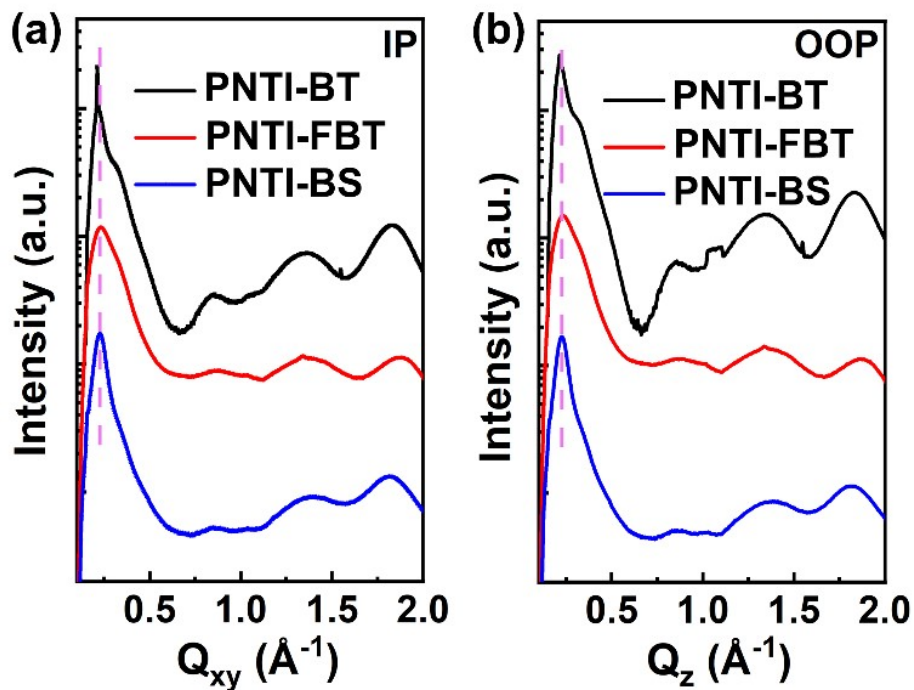


Fig. S10 1D-GIXRD line-cuts of the polymer annealed films deposited on the glass substrate.

11. ^1H NMR spectra and ^{13}C NMR spectra of small molecules and polymers

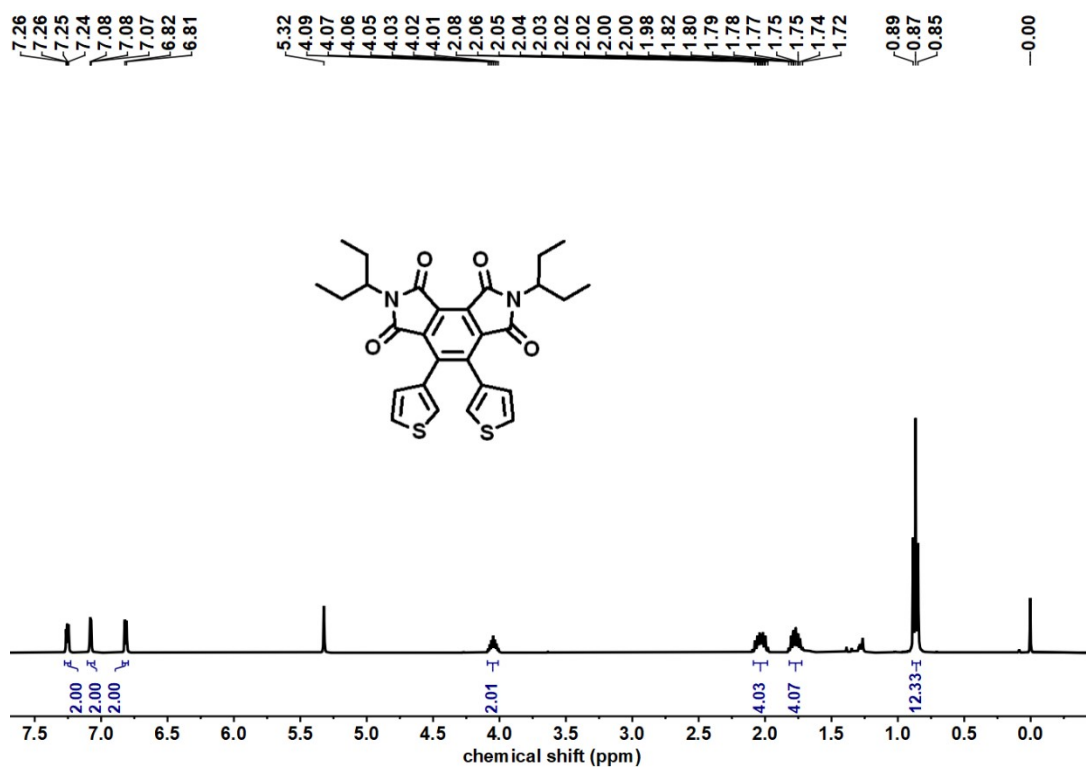


Fig. S11 ^1H NMR spectra of compound 2a in CD_2Cl_2 (298 K).

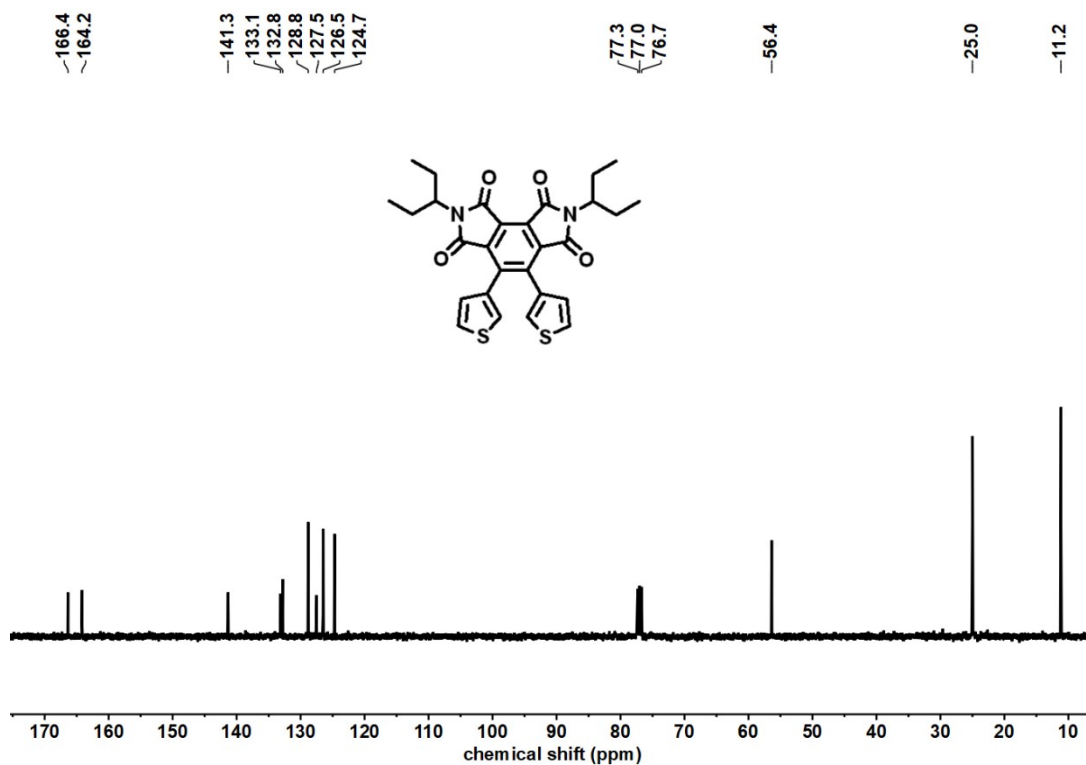


Fig. S12 ^{13}C NMR spectra of compound 2a in CDCl_3 (298 K).

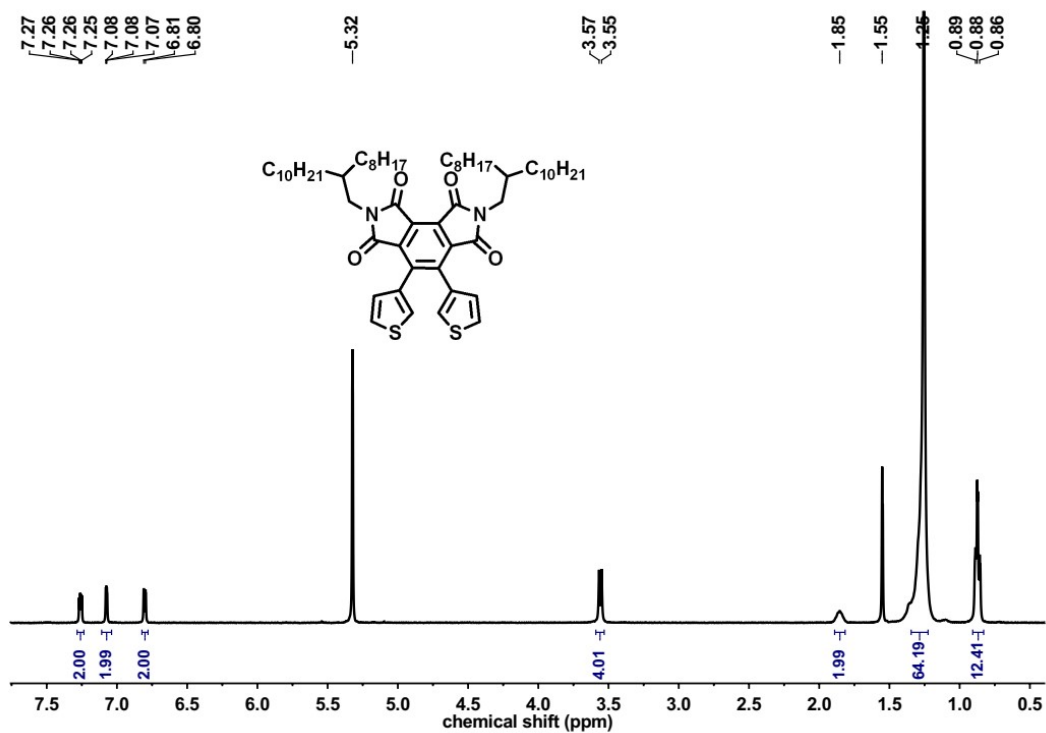


Fig. S13 ^1H NMR spectra of compound 2b in CD_2Cl_2 (298 K).

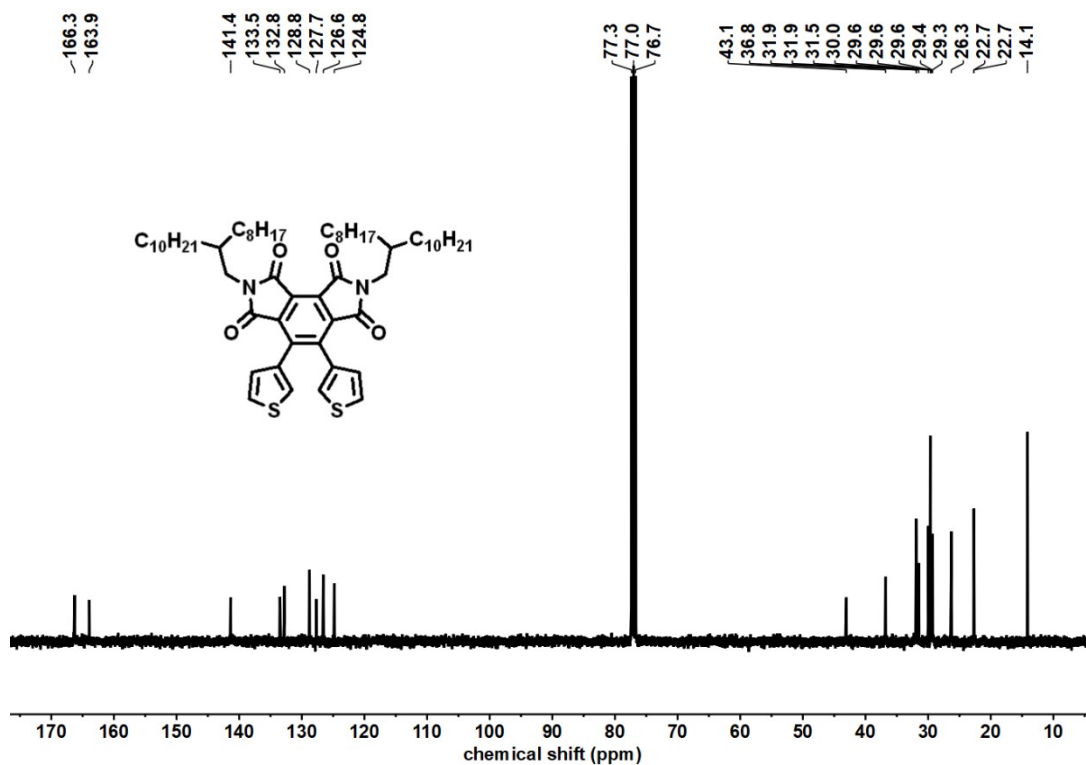


Fig. S14 ¹³CNMR spectra of compound 2b in CDCl₃ (298 K).

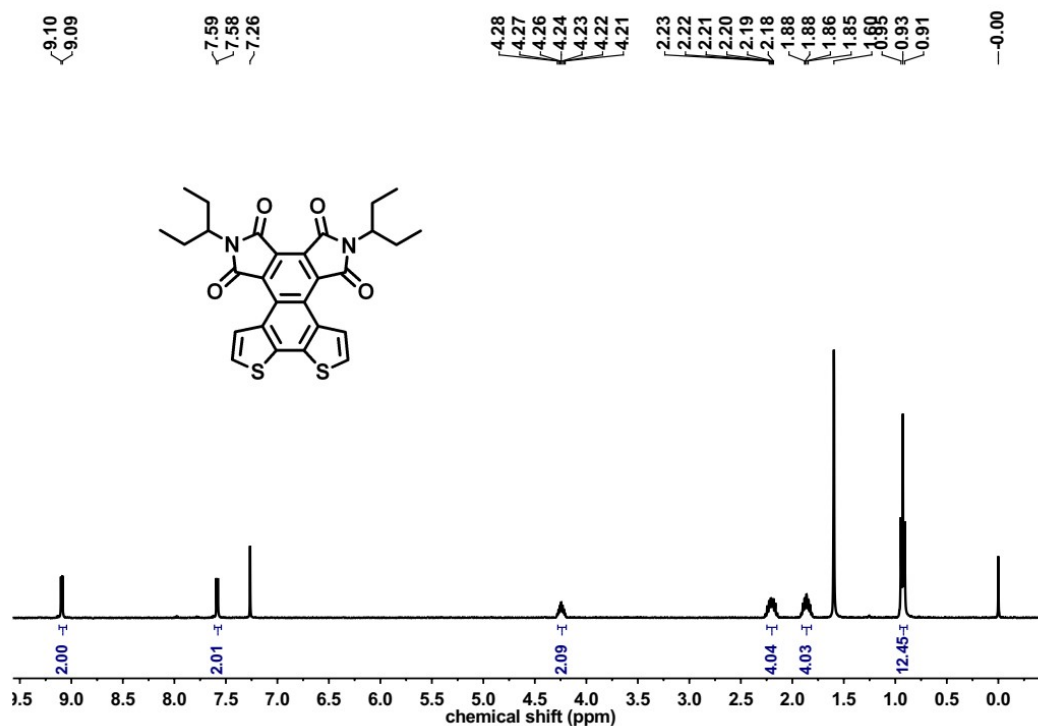


Fig. S15 ¹HNMR spectra of compound 3a in CDCl₃ (298 K).

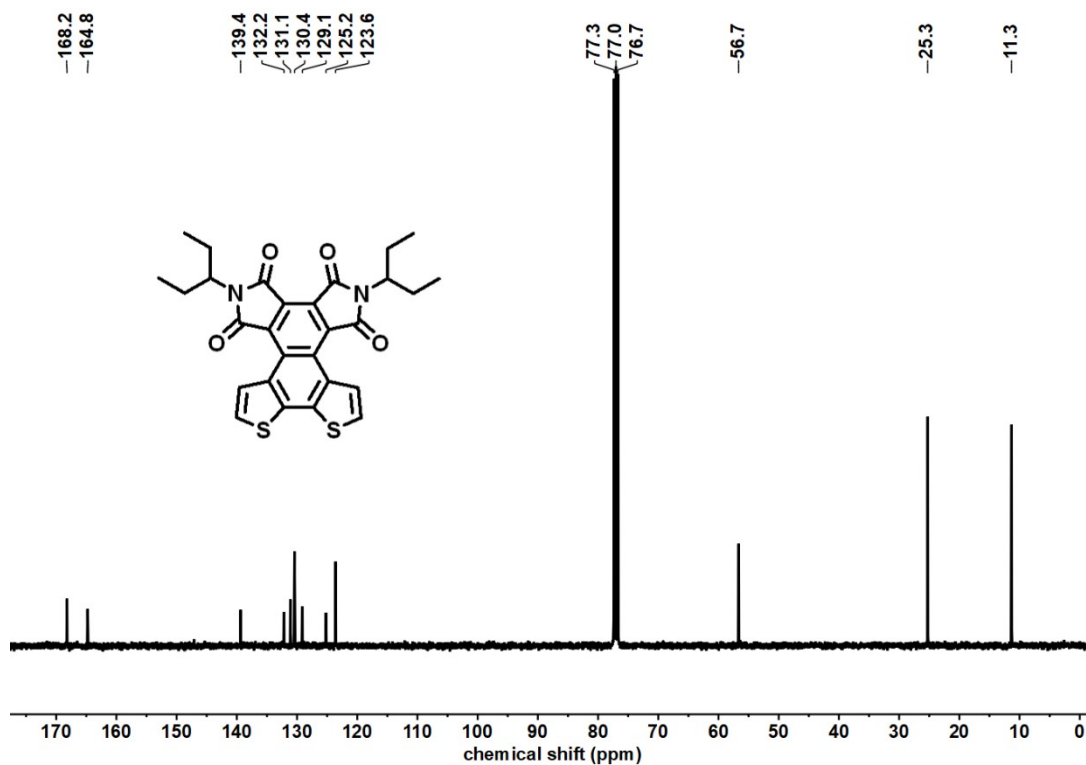


Fig. S16 ^{13}C NMR spectra of compound 3a in CDCl_3 (298 K).

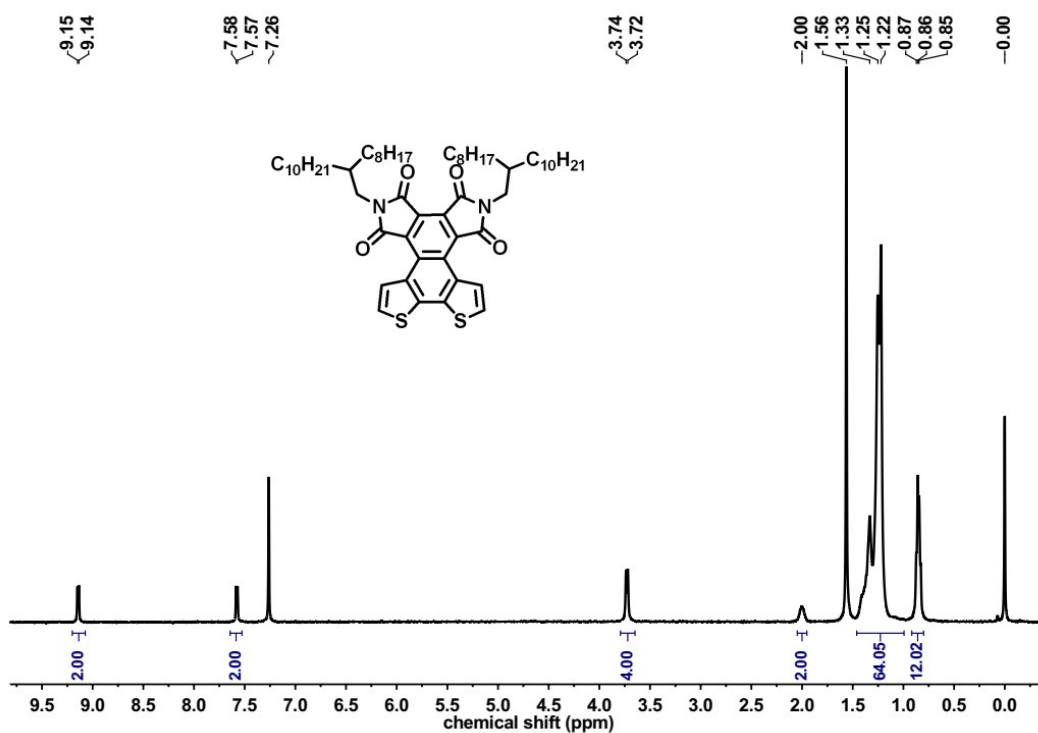


Fig. S17 ^1H NMR spectra of compound 3b in CDCl_3 (298 K).

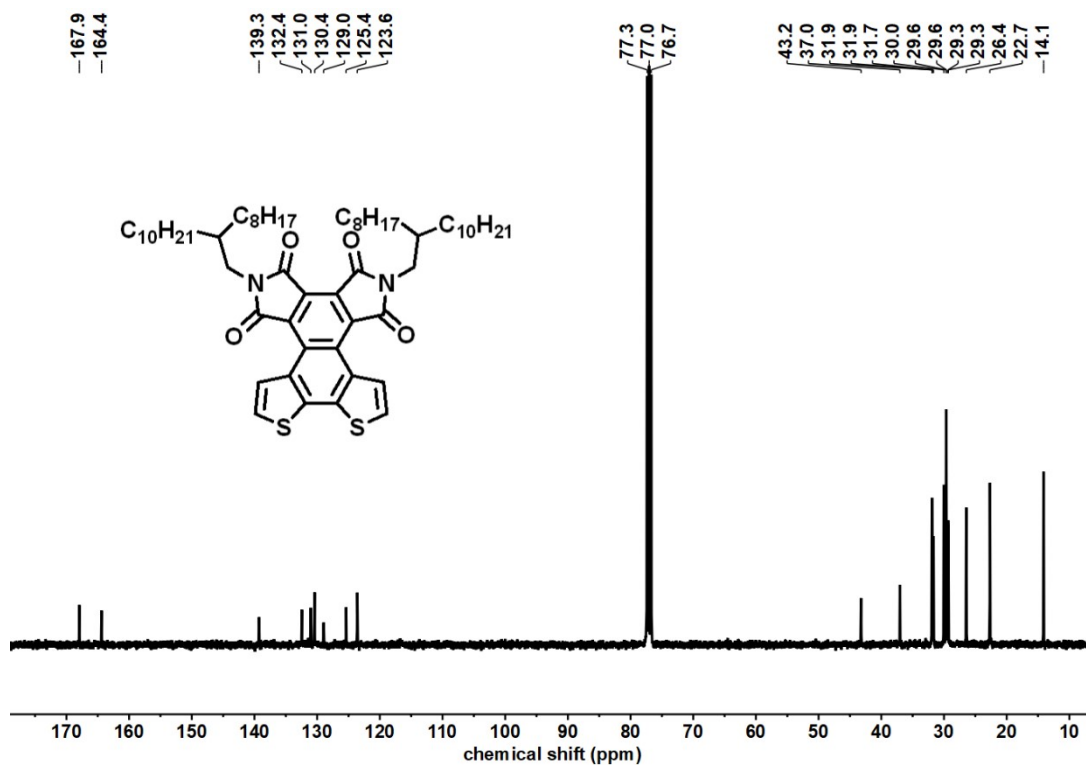


Fig. S18 ^{13}C NMR spectra of compound 3b in CDCl_3 (298 K).

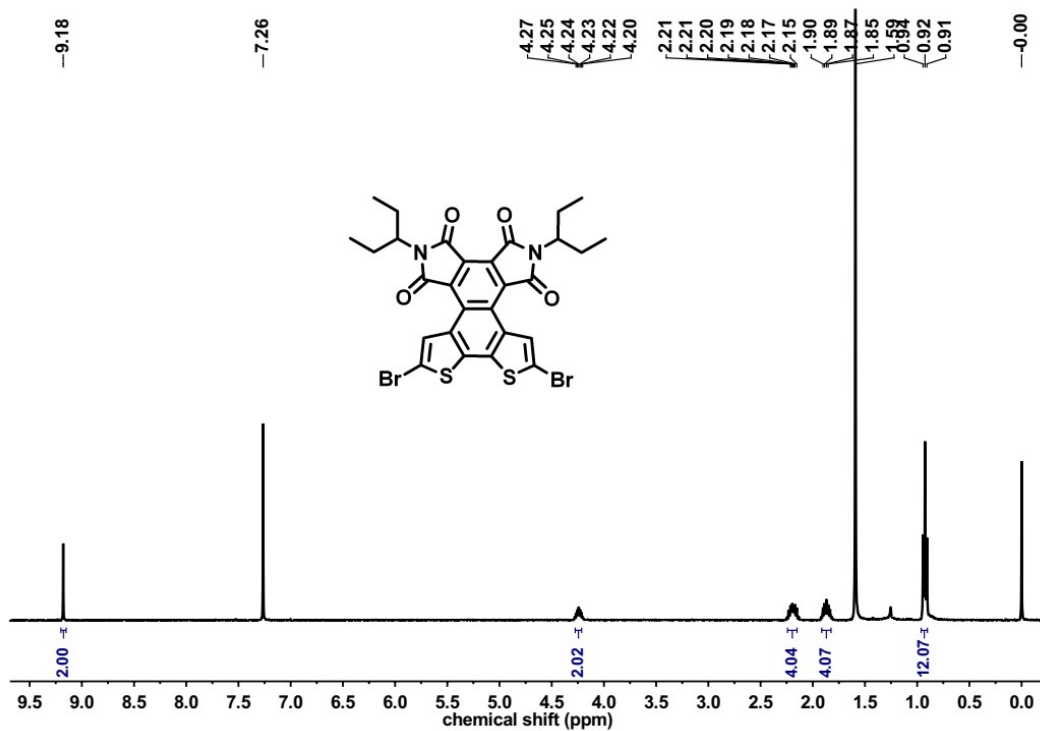


Fig. S19 ^1H NMR spectra of compound 4a in CDCl_3 (298 K).

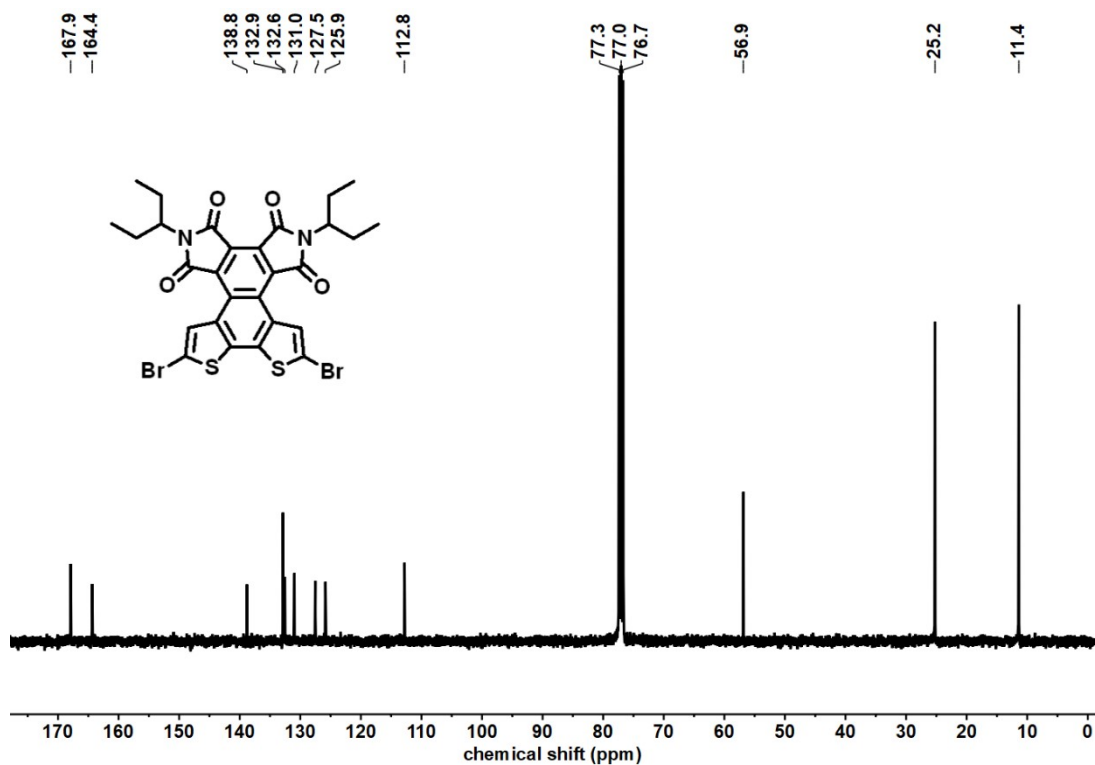


Fig. S20 ^{13}C NMR spectra of compound 4b in CDCl_3 (298 K).

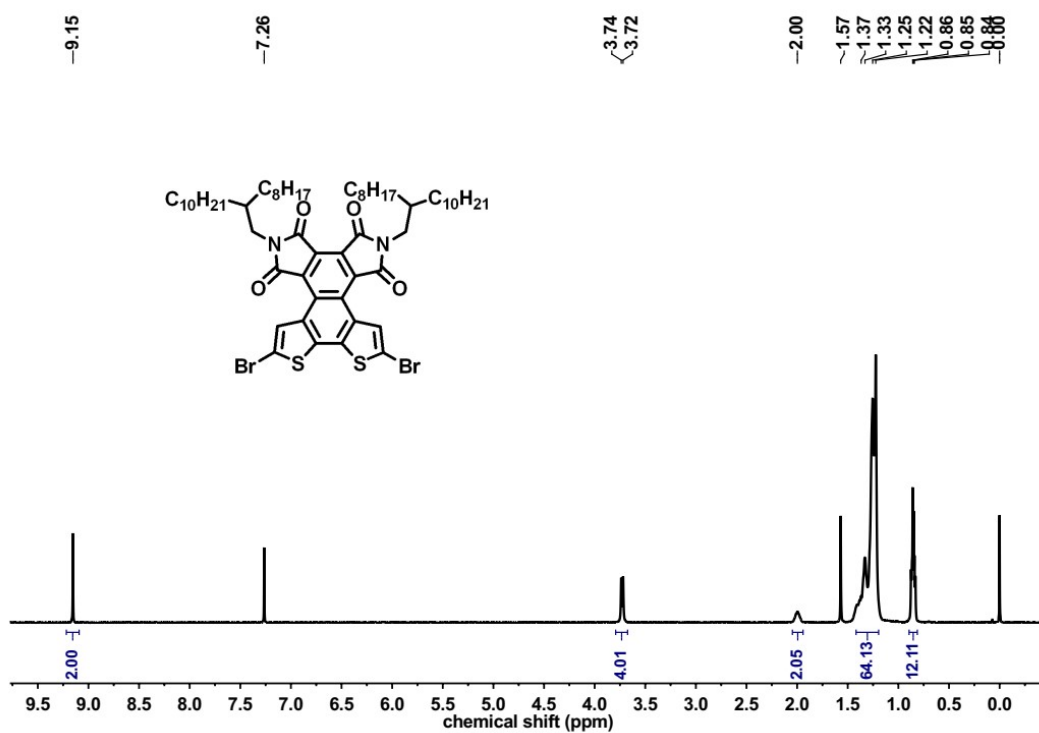


Fig. S21 ^1H NMR spectra of compound 4b in CDCl_3 (313 K).

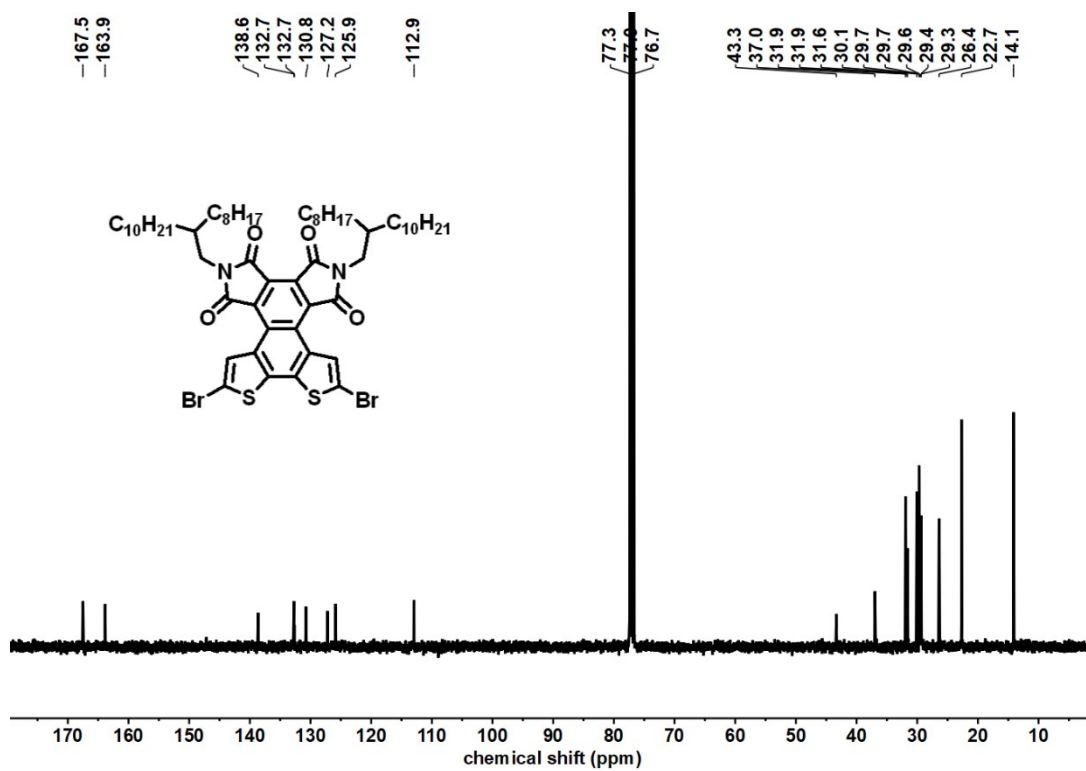


Fig. S22 ¹³CNMR spectra of compound 4b in CDCl₃ (298 K)

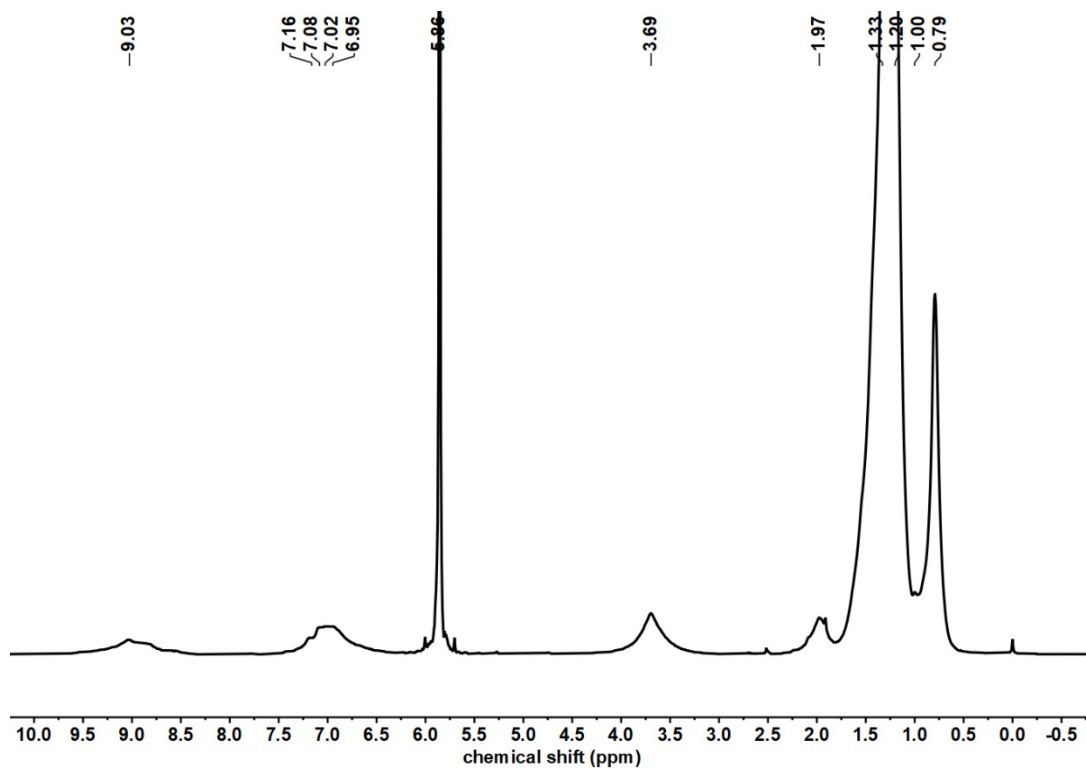


Fig. S23 ¹HNMR spectra of polymer PNTI-BT in C₂D₂Cl₄ (373 K).

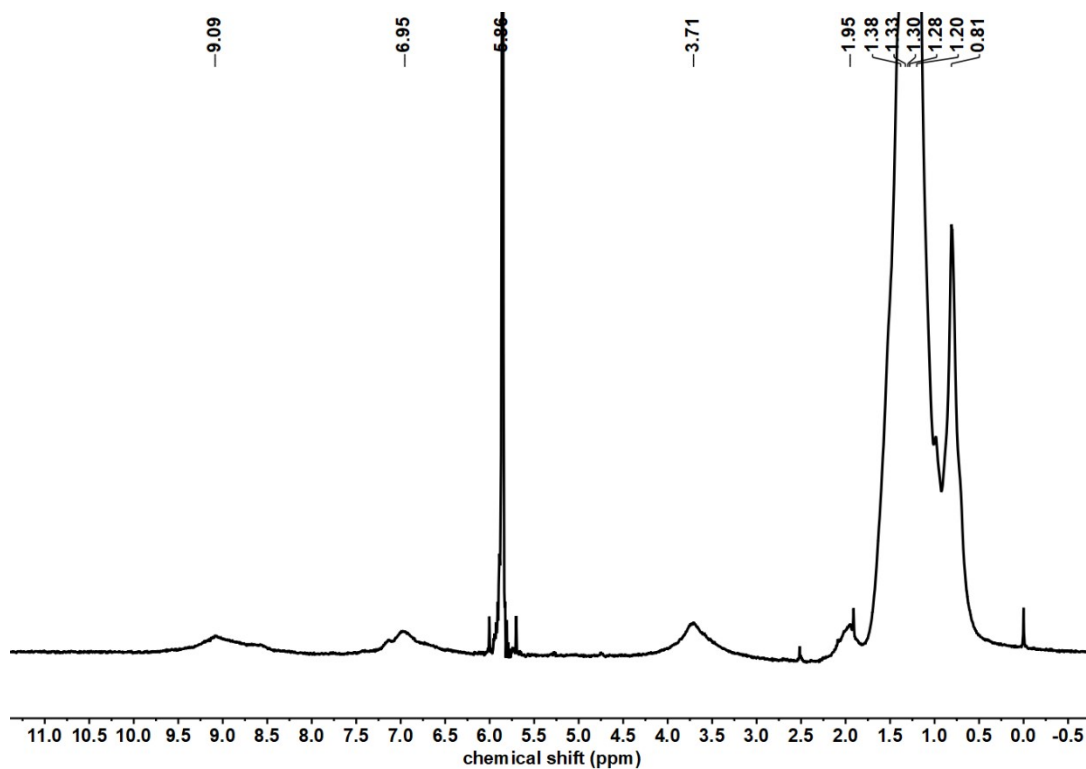


Fig. S24 ^1H NMR spectra of polymer PNTI-FBT in $\text{C}_2\text{D}_2\text{Cl}_4$ (373 K).

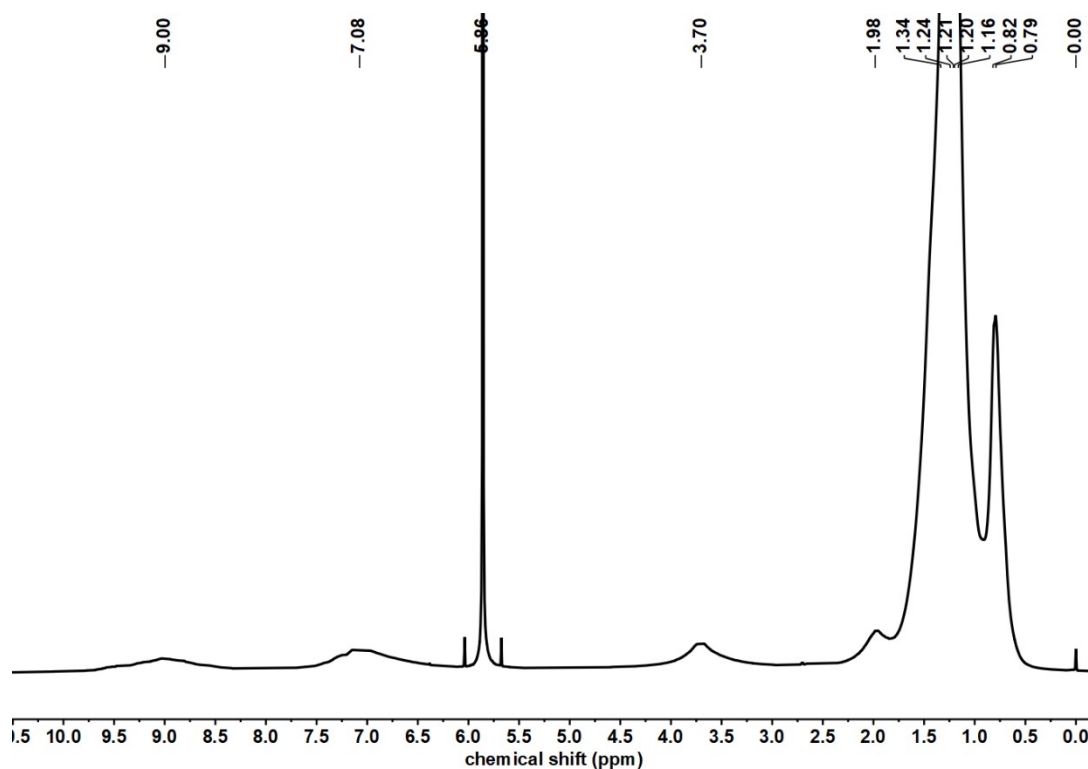


Fig. S25 ^1H NMR spectra of polymer PNTI-BS in $\text{C}_2\text{D}_2\text{Cl}_4$ (373 K).

12. References

- (1) O.V. Dolomanov, L.J. Bourhis, R. J. Gildea, J. A. K. Howard, H. Puschmann, *J. Appl. Cryst.*, **2009**, *42*, 339–341.
- (2) G. M. Sheldrick, *Acta Cryst.*, **2008**, *A64*, 112–122.
- (3) G. M. Sheldrick, *Acta Cryst.*, **2015**, *C71*, 3–8.
- (4) M. J. Frisch, et al. Gaussian 09, Revision B.04; Gaussian, Inc.: Pittsburgh, PA, 2009.
- (5) C. Adamo, V. Barone, *J. Chem. Phys.*, **1999**, *110*, 6158–6170.
- (6) J. Tomasi, B. Mennucci, R. Cammi, *Chem. Rev.*, **2005**, *105*, 2999–3093.
- (7) Y. Zhao, C. A. Di, X. K. Gao, Y. B. Hu, Y. L. Guo, L. Zhang, Y. Q. Liu, Z. H. Wang, W. P. Hu, D. B. Zhu. *Adv. Mater.*, **2011**, *23*, 2448–2453.